



HAL
open science

Contribution to modeling of hydrogen effect on oxygen diffusion in Zy-4 alloy during high temperature steam oxidation.

Benoît Mazères, Clara Desgranges, Caroline Toffolon-Masclat, Daniel Monceau

► To cite this version:

Benoît Mazères, Clara Desgranges, Caroline Toffolon-Masclat, Daniel Monceau. Contribution to modeling of hydrogen effect on oxygen diffusion in Zy-4 alloy during high temperature steam oxidation.. Oxidation of Metals, 2013, 79 (1-2), pp.121-133. 10.1007/s11085-012-9335-1 . hal-03526548

HAL Id: hal-03526548

<https://hal.science/hal-03526548>

Submitted on 14 Jan 2022

HAL is a multi-disciplinary open access archive for the deposit and dissemination of scientific research documents, whether they are published or not. The documents may come from teaching and research institutions in France or abroad, or from public or private research centers.

L'archive ouverte pluridisciplinaire **HAL**, est destinée au dépôt et à la diffusion de documents scientifiques de niveau recherche, publiés ou non, émanant des établissements d'enseignement et de recherche français ou étrangers, des laboratoires publics ou privés.



Open Archive TOULOUSE Archive Ouverte (OATAO)

OATAO is an open access repository that collects the work of Toulouse researchers and makes it freely available over the web where possible.

This is an author-deposited version published in : <http://oatao.univ-toulouse.fr/>
Eprints ID : 8781

To link to this article : DOI:10.1007/s11085-012-9335-1

URL : <http://dx.doi.org/10.1007/s11085-012-9335-1>

To cite this version : Mazères, Benoît and Desgranges, Clara and Toffolon-Masclat, Caroline and Monceau, Daniel *Contribution to modeling of hydrogen effect on oxygen diffusion in Zy-4 alloy during high temperature steam oxidation.* (2013) Oxidation of Metals, vol. 79 (n° 1-2). pp. 121-133. ISSN 0030-770X

Any correspondence concerning this service should be sent to the repository administrator: staff-oatao@listes-diff.inp-toulouse.fr

Contribution to Modeling of Hydrogen Effect on Oxygen Diffusion in Zy-4 Alloy During High Temperature Steam Oxidation

Benoît Mazères · Clara Desgranges ·
Caroline Toffolon-Masclat · Daniel Monceau

Abstract Previous studies have shown that the numerical model EKINOX-Zr was able to simulate with accuracy oxide growth and oxygen diffusion into the matrix during high-temperature oxidation of Zy-4. In this study, the aim of the development was to evaluate if the observed effect of hydrogen cladding content on the increase of oxygen solubility in the high-temperature β_{Zr} was only a thermodynamic effect. Previous experimental studies have shown that hydrogen induces an evolution of equilibrium oxygen concentration at the α_{Zr}/β_{Zr} interface. The present work showed that EKINOX-Zr linked with the thermodynamic database Zircobase reproduced the evolution induced by hydrogen during the high-temperature steam oxidation. However, the results showed also that additional studies are necessary to better understand hydrogen behavior during high-temperature oxidation of Zr.

Keywords Zy-4 · Zr · High-temperature · Oxidation · Modeling · Numerical simulation

B. Mazères · C. Desgranges (✉)
CEA, DEN, DPC, SCCME, Laboratoire d'Etude de la Corrosion Non Aqueuse,
91191 Gif-Sur-Yvette, France
e-mail: clara.desgranges@cea.fr

B. Mazères
e-mail: benoit.mazeres@cea.fr

C. Toffolon-Masclat
CEA, DEN, DMN, SRMA, Laboratoire d'Analyse Microstructurale des Matériaux,
91191 Gif-Sur-Yvette, France
e-mail: caroline.toffolon@cea.fr

D. Monceau
Institut Carnot CIRIMAT, ENSIACET, 4 Allée Emile Monso, BP 44632, 31030 Toulouse Cedex 4,
France
e-mail: daniel.monceau@ensiacet.fr

Nomenclature

EPMA	Electron probe micro analyse
$\frac{dx_i}{dt}$	is the metal/oxide interface velocity
$\frac{dx_j}{dt}$	is the α_{Zr}/β_{Zr} interface velocity
$PBR = 1,56$	is the Pilling–Bedworth ratio between Zr metal matrix and the associated oxide
D_{ox}	is the oxygen coefficient diffusion in the oxide
D_α	is the oxygen coefficient diffusion in $\alpha_{Zr}(O)$
D_β	is the oxygen coefficient diffusion in β_{Zr}
J	is the oxygen flux
c	is the oxygen concentration
t	is the time
$J_{V_k}^n$	is the anionic vacancy flux from slab n to $n + 1$
$D_{V_k}^n$	is the anionic vacancy diffusion vacancies in the slab n
$X_{V_k}^{n+1}$	is the anionic vacancy concentration in the slab n
Ω^n	is the molar volume of the slab n
e^n	is the thickness of the slab n
$X_{V_k}^n = \frac{dX_{V_k}^n}{dt}$	is the rate of change of the anionic vacancies concentration
γ	is linked with the oxide type $MO\gamma$
C_{vap}^{ox}	is the oxygen boundary concentration in the oxide at the steam/oxide interface
C_α^{ox}	is the oxygen boundary concentration in the oxide at the metal/oxide interface
C_{α}^z	is the oxygen boundary concentration in $\alpha_{Zr}(O)$ at the metal/oxide interface
C_{β}^z	is the oxygen boundary concentration in $\alpha_{Zr}(O)$ at the $\alpha_{Zr}(O)/\beta_{Zr}$ interface
C_β^z	is the oxygen boundary concentration in β_{Zr} at the $\alpha_{Zr}(O)/\beta_{Zr}$ interface

Introduction

The loss-of-coolant-accident (LOCA) is a hypothetical accidental scenario which could occur in pressurized light water reactor. This scenario is a temperature transient with a maximum peak-temperature up to 1,200 °C. On the one hand, during this transient, cladding tubes, which are made of Zr based alloys, are submitted to an important oxidation coupled with oxygen diffusion into the bulk. On the other hand, under in-service conditions, cladding tubes can pick up hydrogen. Thus, the post-quench behavior of cladding tubes after LOCA is linked with the oxygen and hydrogen diffusion profiles into the bulk. In a recent work performed at room temperature, Brachet et al. [1] have confirmed the existence of a ductile-to-brittle transition in the β_{Zr} phase due to an oxygen concentration superior to 0.4 wt%. This point has to be carefully addressed since cladding tubes constitute the first confinement barrier of nuclear combustible and fission products. During the transient stage of LOCA, these

tubes need to keep external environment safe from nuclear products. Both ZrO_2 and $\alpha_{Zr}(O)$ formed during the transient are brittle oxygen-rich layers. Thus, after quenching, the residual ductility of the cladding tube is maintained by the remaining prior- β_{Zr} phase containing less than 0.4 wt%. Thus, knowing the growth kinetics of $\alpha_{Zr}(O)$ layer and the oxygen diffusion profile into the β_{Zr} phase are some key elements in order to predict the amount of ductile β_{Zr} layer remaining after a LOCA transient regime. Several calculation tools have been developed in order to predict with precision the cladding tube behavior during LOCA transient [2–5]. Estimation of KINetics OXidation model for Zr based alloys (EKINOX-Zr) is one of them. In a first part, a short presentation of the context is given, followed by a presentation of EKINOX-Zr tool. Next, simulation results are compared with experimental data and discussed.

Context

Cladding Tube

The composition of Zircaloy-4 (Zy-4) alloys used for cladding tubes is given in Table 1.

Phase Transformations of the Cladding Tube During LOCA

In regular-service conditions, the Zr-matrix is single phase α_{Zr} . A layer of monoclinic zirconia is formed on the external surface of the cladding tube (Fig. 1a). During LOCA transient, the increasing temperature induces a phase transformation from α_{Zr} to β_{Zr} (Fig. 1b). At the same time, oxygen diffuses via anionic vacancies in the non-stoichiometric zirconia and via interstitial sites in the metallic matrix. Once the solubility limit of oxygen in β_{Zr} is reached, $\alpha_{Zr}(O)$ phase enriched in oxygen grows from the β_{Zr} phase at the metal/oxide interface (Fig. 1c). At the end of the transient regime, the whole cladding tube is quenched. The final microstructure is divided into three different layers (Fig. 1d). A prior- β_{Zr} phase resulting from the high temperature (HT) stable phase β_{Zr} , which contains the major part of the alloying elements Fe, Cr and potentially H; a layer of $\alpha_{Zr}(O)$ phase enriched in oxygen due to its inward massive diffusion and an external zirconia layer.

Framework

Effect of Hydrogen on the Solubility Limit of Oxygen

Experimental investigations performed by Brachet et al. [1] have shown that hydrogen concentrates into β_{Zr} phase after HT oxidation. It was shown that the

Table 1 Composition of Zy-4 alloys [1]

	Sn	Fe	Cr	O	Zr
Zy-4 (wt%)	1.3	0.20	0.11	0.13	Bal.

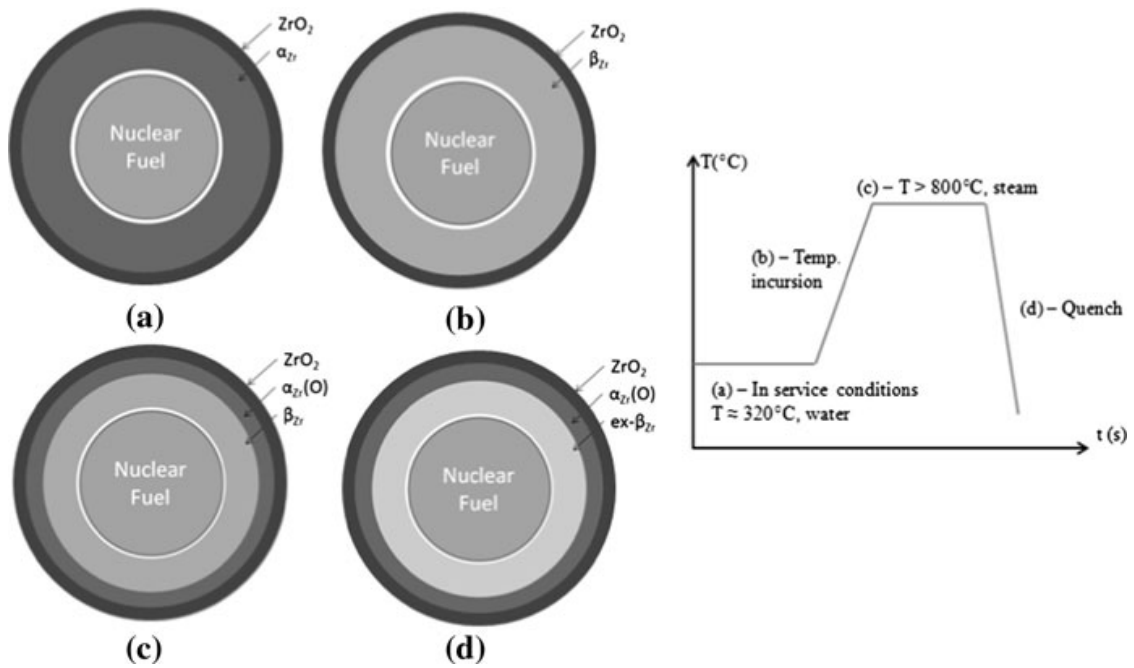


Fig. 1 Schematic of the phase transformations of the cladding tubes during LOCA transient (schematic without scale)

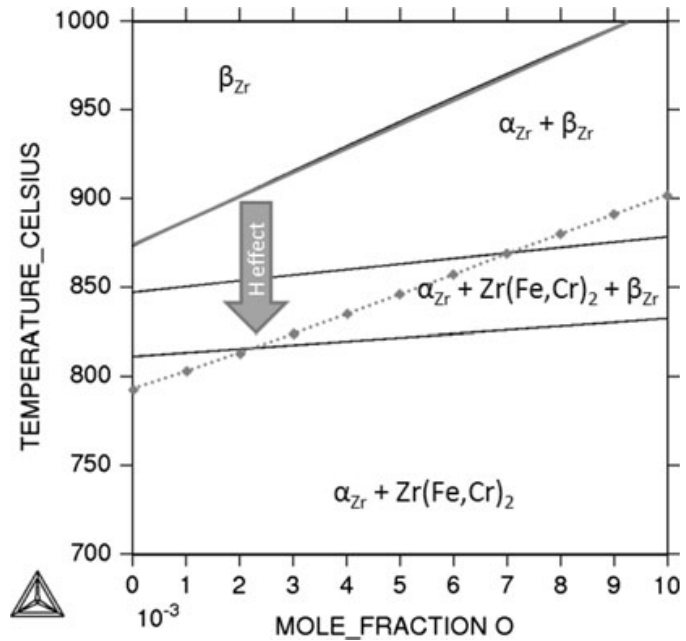
hydrogen concentration increases the solubility limit of oxygen in β_{Zr} . Thermodynamic calculations confirmed this tendency. In this study, calculations were performed with ThermoCalc software and the thermodynamic database Zircobase [6].

The Zircobase database is a thermodynamic database written with Calphad formalism and dedicated to zirconium based systems. It has been developed for the last decade at CEA. Calculations were done considering the Zy-4 chemical composition given in Table 1 plus a hydrogen additional content. Figure 2 shows that the increase of the solubility limit of oxygen is correctly reproduced by thermodynamic calculations [7].

EKINOX-Zr Contribution

EKINOX-Zr tool is an adaptation of a former calculation tool developed to simulate the oxidation of Ni based alloys [8]. EKINOX-Zr development aims to build a numerical model able to predict with accuracy the cladding tubes behavior during HT oxidation. This model has been already presented in details in [9]. This previous work showed that EKINOX-Zr was able to simulate oxygen diffusion and oxide growth during HT oxidation, when considering the Zr–O system. Experimental data were well fitted with simulation results using independent data. In the present paper, EKINOX-Zr calculations are used to evaluate the impact of hydrogen on the cladding tubes oxidation. The objective is to understand if the hydrogen effect is only a thermodynamic effect: that is an increase of the oxygen solubility limit in β_{Zr} . Or if it could also influence the oxygen diffusion coefficient into the β_{Zr} phase. Thus, EKINOX-Zr was improved to take into account the possible roles of

Fig. 2 Zy-4-O diagram. Using Zy-4 composition and Zy-4 composition plus hydrogen content of 5.1 at.%



hydrogen. This has required exchange data between EKINOX-Zr and ThermoCalc (coupled with the Zircobase database) throughout the simulation.

State of the Art

Analytical Solutions

Several analytical models have been developed to predict HT oxidation of metal alloys. Debuigne has proposed an analytical model for zirconium oxidation [10]. In his model, a steady-state hypothesis in a semi-infinite geometry was considered. In a more recent work, Ma et al. [11] have applied Debuigne's analytical model to low-tin Zy-4 steam oxidation between 1,100 and 1,250 °C. Because these analyses made the assumption of a semi-infinite sample, the finite size of cladding tubes could not be simulated. This is a major drawback because of the thickness of nuclear fuel cladding tube is quite limited (close to 600 μm); and because oxygen rapidly reaches the internal surface of the cladding wall.

Other Calculation Tools

Only few numerical simulation tools were developed for Zy-4 oxidation including oxide layer growth and oxygen diffusion at HT in the metallic matrix. Iglesias et al. [2] proposed the FROM (Full Range Oxidation Model) code. FROM is a part of a large platform created to reproduce LOCA conditions in CANada Deuterium Uranium reactors. This code is based on a one dimension diffusion problem with three moving interfaces (vapor/oxide, oxide/ α_{Zr} , α_{Zr}/β_{Zr}).

Oxygen diffusion is governed by Fick's law and interface displacements are controlled by oxygen flux through interfaces. Diffusion equations are solved using a

finite-difference algorithm. The authors ascertain that FROM is able to simulate oxygen diffusion, but published results are only focused on the oxide scale growth. Oxygen saturation in β_{Zr} seems to be treated but it is not described in the article. Berdyshev et al. [3] proposed another numerical model for cladding oxidation as a part of the SVECHA calculation tool package. The numerical model is also based on Fick's law and oxygen flux for interface displacements. The model succeeded in simulating accurately the growth kinetics of $\alpha_{Zr}(O)$ phase with special consideration of oxygen boundary conditions. As for the FROM presentation, SVECHA is focused on growth kinetics of oxide layer and $\alpha_{Zr}(O)$, and does not show any oxygen diffusion profile in the whole cladding wall. Since 2006, the French *Institut de Radioprotection et de Sûreté Nucléaire* (IRSN) has developed the DIFFOX model in order to describe the cladding tube during LOCA transient [4]. DIFFOX is able to simulate double face oxidation of cladding tubes with different conditions on each face. DIFFOX considers a multi-phased oxide layer which is composed of tetragonal and monoclinic zirconia. The authors claim that DIFFOX simulations correctly fit experimental data. Even if the influence of hydrogen seems to be treated by DIFFOX, only one oxygen profile is published while twenty-one experimentations were performed over three temperatures. Furthermore, this oxygen profile shows a significant difference between $\alpha_{Zr}(O)$ thickness measured and calculated by DIFFOX. At last Xiaoqiang et al. [5] have recently presented a model for cladding oxidation during LOCA. This model is based on diffusion equations and considers two different sub-layers to describe zirconia oxide scale. Results show a little discrepancy between zirconia thicknesses calculated and measured.

EKINOX-Zr

General Description

In order to simulate cladding tube behavior during HT oxidation, a set of hypotheses and simplifications are assumed in EKINOX-Zr tool [9]. The problem is modeled in a 1-dimension planar geometry with three moving interfaces: vapor/oxide, oxide/ α_{Zr} , α_{Zr}/β_{Zr} (Fig. 2). Hypotheses are given below:

1. The system is always constituted of three phases: oxide, $\alpha_{Zr}(O)$ phase and β_{Zr} phase.
2. The only diffusing species is oxygen (hydrogen diffuses much faster than oxygen so that no gradient of hydrogen concentration appears in the system).
3. In zirconia, either monoclinic or tetragonal, oxygen is diffusing via anionic vacancies. In the metallic matrix, oxygen diffuses via interstitial sites.
4. Only volume diffusion is considered.
5. Oxygen concentrations at interfaces are always at the equilibrium.
6. In each phase, oxygen diffusion coefficient is only dependent of temperature.

In order to solve numerically the set of equations presented below, the cladding tube is divided into n slabs (Fig. 3). A zero oxygen flux is set at the internal surface of the cladding tube, thus a finite dimension of the cladding and a simple face

oxidation can be considered (Fig. 3). Oxygen boundary concentrations, which are shown in (Fig. 3), are deduced from hypothesis 5 and given as follow (all notations are given at the end of the text):

$$\begin{aligned} C_{ox}(n, t) &= C_{ox/vap}, & C_{ox}(i, t) &= C_{ox/\alpha}, \\ C_{\alpha}(i, t) &= C_{\alpha/ox}, & C_{\alpha}(j, t) &= C_{\alpha/\beta}, \\ C_{\beta}(j, t) &= C_{\beta/\alpha} \end{aligned} \quad (1)$$

Oxygen diffusion, in each phase, can be described by 1-dimension Fick's first and second laws:

$$J = -D \frac{\partial c}{\partial x} \quad \text{and} \quad \frac{\partial J}{\partial x} = -\frac{\partial c}{\partial t} \quad (2)$$

The displacement of α_{Zr}/β_{Zr} interface is governed by the oxygen flux which crosses through the interface. This flux determines the growth kinetics of $\alpha_{Zr}(O)$ layer. Displacement of ox/α_{Zr} interface is governed by the oxygen dissolution in the metal and the oxide growth which is linked to the metal recession.

$$\begin{aligned} (C_{\alpha/\beta} - C_{\beta/\alpha}) \frac{\partial x_j}{\partial t} &= D_{\alpha} \frac{\partial C_{\alpha}}{\partial x} \Big|_j - D_{\beta} \frac{\partial C_{\beta}}{\partial x} \Big|_j \\ (C_{ox/\alpha} - C_{\alpha/ox}) \frac{\partial x_i}{\partial t} &= D_{ox} \frac{\partial C_{ox}}{\partial x} \Big|_i - D_{\alpha} \frac{\partial C_{\alpha}}{\partial x} \Big|_i \end{aligned} \quad (3)$$

Then, the oxide growth is linked to the previous Eq. (3) by:

$$\frac{\partial e}{\partial t} = PBR \frac{\partial x_i}{\partial t} \quad (4)$$

In the oxide, oxygen diffusion from slab to slab is directly deduced from vacancies flux between two slabs, which is calculated as follow:

$$J_{Vo}^p = -\frac{D_{Vo}^p}{\Omega^p} \times \frac{X_{Vo}^{p+1} - X_{Vo}^p}{\frac{e^p - e^{p+1}}{2}} \quad (5)$$

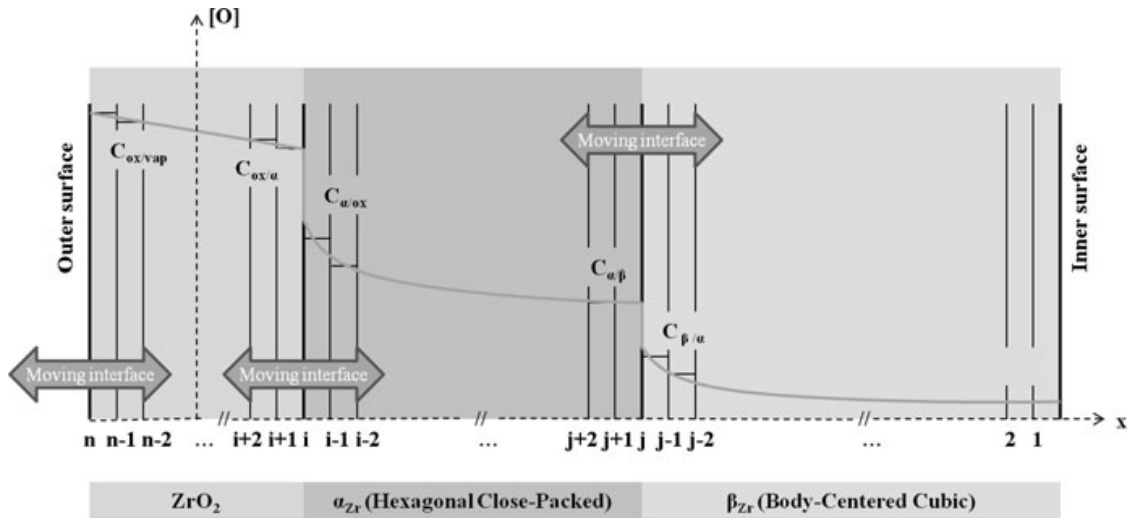


Fig. 3 Schematic of the oxygen diffusion profile into the cladding tube divided into slabs in EKINOX-Zr

The evolution of the oxygen concentration in one slab is governed by the difference of fluxes between two slabs:

$$\dot{X}_{V_o}^p = \frac{dX_{V_o}^p}{dt} = -\Omega^p \times \frac{J_{V_o}^p - J_{V_o}^{p+1}}{e^p} \quad (6)$$

Interface motion, Eq. (3), is numerically described through variations of the slab thickness around interfaces ($j, j + 1$, for the α_{Zr}/β_{Zr} interface and $i, i + 1$ for the metal/oxide interface). Those variations are linked to oxygen mass balance at each interface and to oxygen boundary concentrations. At the same time, oxide growth is associated with a metal recession due to the Pilling–Bedworth ratio of the oxide MO_γ :

$$\frac{de^{j+1}}{dt} = \Omega^{j+1} \times \frac{J_{V_o}^{j-1} - J_{V_o}^{j+1}}{C_{\alpha/\beta} - C_{\beta/\alpha}} \quad \text{and} \quad \frac{de^{i+1}}{dt} = \frac{\Omega^{i+1}}{\gamma} \times \frac{J_{V_o}^{i-1} - J_{V_o}^{i+1}}{C_{ox/\alpha} - C_{\alpha/ox}} \quad (7)$$

A special algorithm for changing increments j and i authorizes interface motion over a large displacement [7].

EKINOX-Zr Improvement

EKINOX-Zr was improved in order to take into account the effect of hydrogen on the solubility limit of oxygen into β_{Zr} phase. As EKINOX-Zr considered only oxygen diffusion, and because the hydrogen diffusion is expected to be much faster than oxygen diffusion, it was decided to consider that the whole hydrogen is concentrated into the β_{Zr} phase as it was concluded in [1]. As a consequence, during HT oxidation process, the internal prior- β_{Zr} layer is enriched progressively in hydrogen. It was necessary to re-calculate oxygen equilibrium concentrations at the α_{Zr}/β_{Zr} interface at each time step of the simulation. For this purpose, EKINOX-Zr was linked to ThermoCalc (coupled with the Zircobase database) via TQ interface.

Thermodynamic Data Set

Oxygen concentrations $C_{\alpha/\beta}$ and $C_{\beta/\alpha}$ were calculated at each iteration at the metal/oxide interface considering a {Zr–O} system and at the α_{Zr}/β_{Zr} interface considering a {Zr–O–H} system. Table 2 summarizes the oxygen diffusion coefficients which are used in EKINOX-Zr. They are obtained from [11]. For each simulation concentrations of oxygen vacancies at both sides of the oxide layer are fixed to the values given in Table 2.

Results

Figure 4a presents the growth kinetics of the oxide layer obtained from experimental data together with the one calculated by EKINOX-Zr for Zy-4 with hydrogen concentration up to 5.1 at.%. Figure 4b presents the oxygen diffusion profiles calculated by EKINOX-Zr at different times. One can clearly see on these

Table 2 Diffusion coefficients [11] and oxygen concentration in zirconia used in EKINOX-Zr

T (°C)	D_{ox} (cm ² /s)	D_{α} (cm ² /s)	D_{β} (cm ² /s)	$[V_O]_{ox/vap}$ (at.%)	$[V_O]_{ox/z}$ (at.%)	$C_{z/ox}$ (at.%)
1,200	9.21×10^{-7}	1.10×10^{-7}	1.55×10^{-6}	1.0×10^{-6}	9.0	30.53

profiles the growth of both oxide and the $\alpha_{Zr}(O)$ layers. The lower profile in black (Fig. 4b) present the initial conditions of the simulation with the assumption of hypothesis 1: two small layer of both oxide and $\alpha_{Zr}(O)$ and the rest of the metallic matrix in β_{Zr} phase.

Portier et al. [12] have done oxidation at 1,200 °C on Zy-4 samples with a hydrogen content close to 5.1 at.%. This study showed that hydrogen has no effect on growth kinetics of the oxide layer. One can see that the calculated parabolic growth of the zirconia layer fits correctly the experimental data. Thus, hydrogen content has also no effect on oxide growth kinetics calculated by EKINOX-Zr.

Issued from [13], Fig. 5a presents oxygen diffusion profiles (rescaled on the β_{Zr} phase) measured using electron probe micro analyse (EPMA) on three Zy-4 samples, one without hydrogen, one with a 1.3 at.% hydrogen content and last one containing 5.1 at.% hydrogen content. Those samples have been oxidized under steam at 1,200 °C during approximately 200s. One can observe the increasing solubility limit of oxygen when increasing the nominal hydrogen content. Oxygen diffusion profiles have been calculated by EKINOX-Zr for the same nominal composition and are compared with those obtained from experimental measurements (Fig. 5b–d) [8, 10]. Oxygen diffusion profiles are only plotted in the metal matrix, the left part corresponds to $\alpha_{Zr}(O)$ phase and the right one to β_{Zr} phase.

The calculated profile for 187s hydrogen-free material and experimental data are in good agreement in β_{Zr} phase (Fig. 5b). The second calculated profile for medium hydrogen content (1.3 at.%) and experimental data are also in good agreement in β_{Zr} phase (Fig. 5c). The last graph shows a large difference between the thickness of

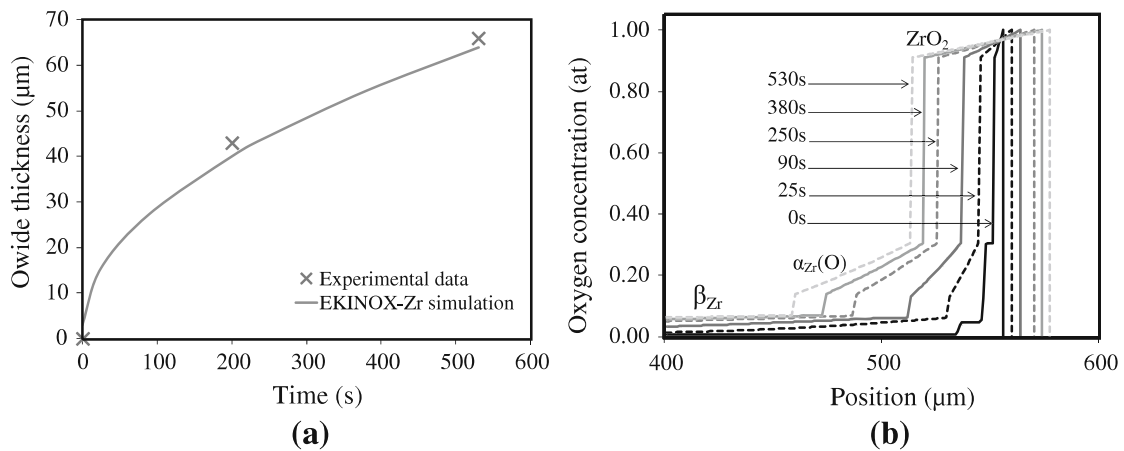


Fig. 4 (a) Comparison between the growth kinetics of the oxide layer for Zy-4 + [H] = 5.1 at.% obtained from experimental data [13] and calculated by EKINOX-Zr. (b) Corresponding global oxygen diffusion profiles calculated with EKINOX-Zr, the outer surface is located on the *right side*

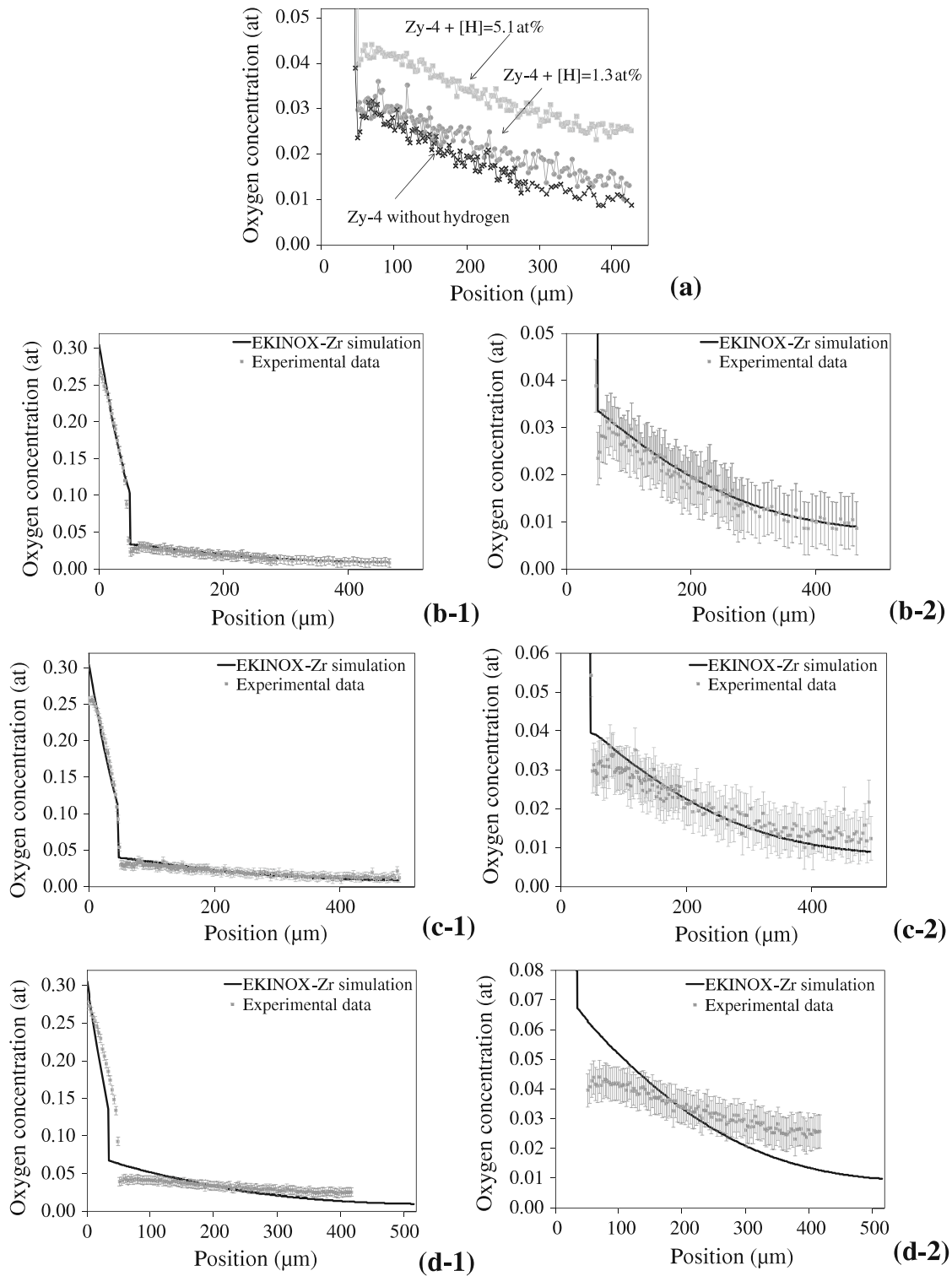


Fig. 5 (a) Issued from [13] EPMA oxygen profiles in β_{Zr} for three nominal H contents. Comparison between oxygen diffusion profiles obtained from experimental data [9, 13] and calculated by EKINOX-Zr (b-1, 2) 0, (c-1, 2) 1.3 at.%, and (d-1, 2) 5.1 at.% of hydrogen. Profiles (b-2), (c-2) and (d-2) correspond respectively to the β_{Zr} phase of profiles (b-1), (c-1) and (d-1). All oxidation durations are about 200 s. For all experimental profiles, the error is about 0.56 at.%

the $\alpha_{\text{Zr}}(\text{O})$ layer measured experimentally and the one calculated with EKINOX-Zr (Fig. 5d). Moreover, oxygen boundary concentrations $C_{\beta/\alpha}$ measured and calculated by EKINOX-Zr differ strongly. As a consequence, the experimental profile is not

Table 3 Hydrogen partitioning between $\alpha_{\text{Zr}}(\text{O})$ and β_{Zr} phases calculated with ThermoCalc

T (°C)	$[\text{H}]_{\text{Zy-4}}$ (at.%)	n_{α}/n_{β} (mol)	$[\text{H}]_{\alpha}$ (at.%)	$[\text{H}]_{\beta}$ (at.%)
1,200	1.3	0.51/0.49	1.21	1.47
1,200	5.1	0.51/0.49	4.32	6.00

Each equilibrium calculations were performed at 1,200 °C with 1 mol of alloy

well reproduced by calculations. In fact, the discrepancy between measured and calculated oxygen diffusion profiles increases with the hydrogen content.

Discussion

The increasing value of the oxygen solubility $C_{\beta/\alpha}$ when increasing the hydrogen content, which was observed in experimental studies, is reproduced by EKINOX-Zr, but is overestimated. Thermodynamic calculations for two different hydrogen contents (Table 3) indicate a hydrogen partitioning between $\alpha_{\text{Zr}}(\text{O})$ and β_{Zr} . It is different from the hypothesis done on hydrogen concentration in the EKINOX-Zr calculations considering that hydrogen is completely concentrated in β_{Zr} , based on experimental data from [1].

Secondly, during calculations, $\alpha_{\text{Zr}}(\text{O})$ grows at the expense of β_{Zr} , in the meantime hydrogen concentrates uniformly into β_{Zr} . Brachet et al. [1] have performed an hydrogen quantitative mapping of oxidized Zy-4 samples with 5.1 at.% hydrogen content (oxidation under steam at 1,200 °C during 615 s). Mapping was done thanks to an electron recoil detection analyser. It revealed a local increase in hydrogen content in the β_{Zr} phase close to the $\alpha_{\text{Zr}}(\text{O})/\beta_{\text{Zr}}$ interface. This local hydrogen enrichment is not considered in EKINOX-Zr, but it may have an effect on the solubility limit of oxygen at this interface. In the same work, thanks to an EPMA, measurements of iron and chromium concentration have been done on same samples. They have shown that iron and chromium are also massively concentrated in β_{Zr} phase during oxidation at 1,200 °C. Thus, one can also wonder if iron and chromium could have an effect on thermodynamic calculations. Eventually, consideration of iron and chromium in thermodynamic calculations shows a very little diminution of the over-estimated value of the solubility limit of oxygen in β_{Zr} phase. However, it is clear that the local enrichment in hydrogen and chromium beneath the $\alpha_{\text{Zr}}(\text{O})/\beta_{\text{Zr}}$ interface, plus the global enrichment of the β_{Zr} phase in iron induce a very particular chemistry beneath the interface which is difficult to evaluate without consideration of the diffusion of all the elements in the system.

Thirdly, the graphics presented in Fig. 5 show that hydrogen concentration increases the difference between calculated $\alpha_{\text{Zr}}(\text{O})$ thicknesses and measured ones. It is not excluded that hydrogen has also an effect on the oxygen diffusion coefficients. Such effect has not been introduced in the present calculations. Furthermore, in EKINOX-Zr, oxygen diffusion coefficients are independent from

oxygen concentration. One can observe in Fig. 5a, b and c, that the experimental oxygen diffusion profile in $\alpha_{\text{Zr}}(\text{O})$ are convex whereas calculated profiles are concave. That could be due to an effect of oxygen concentration on its diffusion coefficient by increasing the oxygen diffusion when oxygen concentration increases. Hence, it appears that it is not fully justified to neglect the variation of oxygen diffusion with oxygen and hydrogen contents. Moreover, the diffusion of the other alloying elements can also have an influence on the oxygen diffusion profile. In fact, recent work [14] has shown that tin, iron and chromium have a particular behaviour during oxidation at 1,200 °C in a steam environment. Tin presents no significant partitioning between $\alpha_{\text{Zr}}(\text{O})$ and β_{Zr} , despite its well known $\alpha_{\text{Zr}}(\text{O})$ -stabilizer behavior, whereas iron, chromium and hydrogen are clearly β_{Zr} -stabilizer elements. Brachet et al. also showed in [16] that iron and chromium also concentration in β_{Zr} at HT with local enrichment of Cr close to the $\alpha_{\text{Zr}}(\text{O})/\beta_{\text{Zr}}$ interface. Diffusion coefficients of tin, iron and chromium have been determined in the β_{Zr} phase in [15]. At 1,200 °C in β_{Zr} phase, tin, chromium and iron diffusion coefficient are respectively equal to 8.10×10^{-13} , 7.40×10^{-12} and 9.00×10^{-11} cm²/s. Then, they diffuse very slowly in comparison to the oxygen diffusion, so they could be neglected in EKINOX-Zr calculations when considering short time oxidation. Hydrogen diffusion coefficient has been determined in [15]: 3.04×10^{-4} cm²/s. EKINOX-Zr being based on an explicit finite difference algorithm, the time step for integration is based on the fastest diffusing element. Considering hydrogen diffusion in the calculations could be done but should lead to long duration calculations. Hence, in next works, considering hydrogen partitioning in a more accurate manner than done for these first calculations could be a more efficient way to improve calculations.

Conclusions

The first simulations coupling diffusion of oxygen and thermodynamic effect of hydrogen, in the system {Zr–O–H} show that the experimental evolution tendencies are well reproduced with EKINOX-Zr calculations, but are over-estimated. One can conclude that the effect of hydrogen on oxygen diffusion may not only be a thermodynamic one. Thus, the simplistic hypotheses that have been set in EKINOX-Zr on the hydrogen behavior are not sufficient for an appropriate description of the hydrogen effect. It is possible that the effects of hydrogen are mixed with the possible effects of chromium and iron showing some local enrichment at the $\alpha_{\text{Zr}}(\text{O})/\beta_{\text{Zr}}$ interface. It would be interesting to consider chromium and iron in the thermodynamic calculations for future developments of EKINOX-Zr.

Acknowledgments The authors would like to thank J.-C. Brachet and V. Vandenberghe from CEA Saclay for their helpful discussions. This study was funded by AREVA and EDF.

References

1. J.-C. Brachet, V. Vandenberghe, L. Portier, D. Gilbon, A. Lesbros, N. Waeckel, and J.-P. Mardon, *Journal of ASTM international*, **5**, no. 5, Paper ID JAI101116 (2008).

2. F. C. Iglesias, D. B. Duncan, S. Sagat and H. E. Sills, *Journal of Nuclear Materials* **130**, 1985 (36).
3. A. V. Berdyshev and M. S. Veshchunov, *Proceeding of Nuclear Safety Institute (IBRAE-RAS)*, vol. 1, pp. 6–14 (2010).
4. C. Duriez, S. Guilbert, A. Stern, C. Grandjean, L. Belovsky, J. Desquines, *Journal of ASTM International*, **2**, no 8, Paper ID JAI103156 (2010).
5. H. Xiaoqiang, Y. Hongxing, J. Guangming. in *2011 Water Reactor fuel Performance Meeting*. Conference Proceeding T3-040. (Chengdu, China, Sept 11–14, 2011).
6. N. Dupin, I. Ansara, C. Servant, C. Toffolon, C. Lemaignan and J.-C. Brachet, *Journal of Nuclear Materials* **275**, 2004 (287).
7. C. Toffolon-Masclat, C. Desgranges, C. Corvalan-Moya and J. C. Brachet, *Solid State Phenomena* **172**, 2011 (652).
8. C. Desgranges, N. Bertrand, K. Abbas, D. Monceau and D. Poquillon, *Materials Science Forum* **461**, 2004 (481).
9. C. Corvalán-Moya, C. Desgranges, C. Toffolon-Masclat, C. Servant, and J.C. Brachet, *Journal of Nuclear Materials*. **400**, 196 (2010).
10. J. Debuigne, *Contribution to Study of Zirconium Oxidation and oxygen Diffusion into the Oxide and the Metal*, PhD Thesis, Faculté des sciences de Paris (1966).
11. X. Ma, C. Toffolon, T. Guilbert, D. Hamon and J.-C. Brachet, *Journal of Nuclear Materials* **377**, 2008 (359).
12. L. Portier, T. Bredel, J.-C. Brachet, V. Vandenberghe, J.-P. Mardon and A. Lesbros. *Journal of ASTM international*, **2**, no 2, Paper ID JAI12468 (2005).
13. M. Le Saux, J.-C. Brachet, V. Vandenberghe, D. Gilbon, J.-P. Mardon, B. Sebbari, in *2011 Water Reactor fuel Performance Meeting*. Conference Proceeding T3-040. (Chengdu, China, Sept 11–14, 2011).
14. J.-C. Brachet, C. Toffolon, D. Hamon, T. Guilbert, G. Trego, J. Jourdan, A. Stern and C. Raespaet, *Solid State Phenomena* **172**, 2011 (753).
15. H. Mehrer. *Diffusion in Solids Metals and Alloys*, Vol. 26. Landolt-Börnstein collection. (Springer, Berlin, 1990), p. 100 and 515.
16. J.-C. Brachet, J. Pelchat, D. Hamon, R. Maury, P. Jacques, J.-P. Mardon, in *TCM on fuel behavior under transient and LOCA conditions*. Conference Proceeding, International Atomic Energy Agency (Halden, Sept 10–14, 2001).